



The power of the Invitrogen™ immunoassay portfolio—
your advantage on the road to discovery

Let's go

invitrogen
by Thermo Fisher Scientific



CSF-1R–Dependent Lethal Hepatotoxicity When Agonistic CD40 Antibody Is Given before but Not after Chemotherapy

This information is current as
of December 12, 2017.

Katelyn T. Byrne, Nathan H. Leisenring, David L. Bajor and
Robert H. Vonderheide

J Immunol 2016; 197:179-187; Prepublished online 23 May
2016;

doi: 10.4049/jimmunol.1600146

<http://www.jimmunol.org/content/197/1/179>

Supplementary Material <http://www.jimmunol.org/content/suppl/2016/05/20/jimmunol.1600146.DCSupplemental>

Why *The JI*?

- **Rapid Reviews! 30 days*** from submission to initial decision
- **No Triage!** Every submission reviewed by practicing scientists
- **Speedy Publication!** 4 weeks from acceptance to publication

**average*

References This article **cites 41 articles**, 20 of which you can access for free at:
<http://www.jimmunol.org/content/197/1/179.full#ref-list-1>

Subscription Information about subscribing to *The Journal of Immunology* is online at:
<http://jimmunol.org/subscription>

Permissions Submit copyright permission requests at:
<http://www.aai.org/About/Publications/JI/copyright.html>

Email Alerts Receive free email-alerts when new articles cite this article. Sign up at:
<http://jimmunol.org/alerts>

The Journal of Immunology is published twice each month by
The American Association of Immunologists, Inc.,
1451 Rockville Pike, Suite 650, Rockville, MD 20852
Copyright © 2016 by The American Association of
Immunologists, Inc. All rights reserved.
Print ISSN: 0022-1767 Online ISSN: 1550-6606.



CSF-1R-Dependent Lethal Hepatotoxicity When Agonistic CD40 Antibody Is Given before but Not after Chemotherapy

Katelyn T. Byrne, Nathan H. Leisenring, David L. Bajor, and Robert H. Vonderheide

Cancer immunotherapies are increasingly effective in the clinic, especially immune checkpoint blockade delivered to patients who have T cell-infiltrated tumors. Agonistic CD40 mAb promotes stromal degradation and, in combination with chemotherapy, drives T cell infiltration and de novo responses against tumors, rendering resistant tumors susceptible to current immunotherapies. Partnering anti-CD40 with different treatments is an attractive approach for the next phase of cancer immunotherapies, with a number of clinical trials using anti-CD40 combinations ongoing, but the optimal therapeutic regimens with anti-CD40 are not well understood. Pancreatic ductal adenocarcinoma (PDA) is classically resistant to immunotherapy and lacks baseline T cell infiltration. In this study, we used a tumor cell line derived from a genetically engineered mouse model of PDA to investigate alterations in the sequence of anti-CD40 and chemotherapy as an approach to enhance pharmacological delivery of chemotherapy. Unexpectedly, despite our previous studies showing anti-CD40 treatment after chemotherapy is safe in both mice and patients with PDA, we report in this article that anti-CD40 administration <3 d in advance of chemotherapy is lethal in more than half of treated C57BL/6 mice. Anti-CD40 treatment 2 or 3 d before chemotherapy resulted in significantly increased populations of both activated myeloid cells and macrophages and lethal hepatotoxicity. Liver damage was fully abrogated when macrophage activation was blocked using anti-CSF-1R mAb. These studies highlight the dual nature of CD40 in activating both macrophages and T cell responses, and the need for preclinical investigation of optimal anti-CD40 treatment regimens for safe design of clinical trials. *The Journal of Immunology*, 2016, 197: 179–187.

Immunotherapies such as anti-programmed cell death-1 (PD-1)/ligand-1 and anti-CTLA-4 have shown significant clinical efficacy in some patients with certain cancers, including those with metastatic disease (1–3). However, these therapies are most often successful in the subset of patients who have an ongoing immune response against the tumor and are less effective against tumors that lack baseline T cell infiltration (4). Patients with poorly infiltrated tumors have a much lower prognosis, even for classically immunogenic cancers such as melanoma (5). Pancreatic ductal adenocarcinoma (PDA) is a canonical example of a poorly immunogenic tumor because it largely lacks strong neo-epitopes (6–8) and T cell infiltration, correlating with a dismal 5-y survival rate of <5%. Gemcitabine (Gem) is part of a standard of care for patients with PDA but serves to extend overall survival by only a few weeks to months (9). Patients with PDA are resistant to CTLA-4 or PD-1 Ab therapy (1, 10, 11). Thus, improved treatments that are effective in tumors that lack endogenous T cell infiltration are needed in the clinic.

Agonistic CD40 mAb functions analogous to CD40-ligand in vivo, activating and maturing APCs (12–14). In some highly immunogenic mouse models of cancers, anti-CD40 therapy results in T cell-mediated tumor regressions (15), but in other models of solid tumors, anti-CD40 alone is not sufficient to mediate antitumor T cell responses (16, 17). Indeed, using the genetically engineered $Kras^{LSL-G12D/+}$, $Trp53^{LSL-R172H/+}$, $Pdx1-Cre$ (KPC) mouse model of PDA, in which oncogenic $Kras^{G12D}$ and mutant $p53^{R172H}$ are under the control of Cre recombinase specifically expressed in the pancreas (18), we have shown that anti-CD40 alone fails to prime T cell responses against PDA (16). KPC mice faithfully recapitulate key features of human disease, including a dearth of nonsynonymous mutations [similar to other $Kras$ -induced mouse models of cancer (19)] and minimal effector T cell infiltration (20). The lack of T cells in PDA tumors correlates with resistance to current immunotherapies, including anti-PD-1 and anti-CTLA-4 in mice (21), as is also observed in patients with PDA (1). However, agonistic anti-CD40 activates dendritic cells and is capable of driving T cell infiltration and T cell-dependent regression of established tumors when administered 48 h after treatment with Gem (17, 22), and it is sufficient to render PDA susceptible to anti-PD-1/anti-CTLA-4 treatment (21). Gem is hypothesized to augment anti-CD40 therapy by killing tumor cells and liberating tumor Ags that are then picked up and presented by APCs (17). Thus, anti-CD40 is an immunotherapy capable of converting tumors devoid of T cells (and refractory to anti-PD-1/anti-CTLA-4) to a tumor that is sensitive to T cell-mediated destruction, potentially filling a void in the clinical toolbox for treating patients with cancer.

In addition to the ability of anti-CD40 to activate APCs and prime T cell responses, we have shown that anti-CD40 stimulation alters tumor stroma and activates macrophages to become tumoricidal (16). Therefore, anti-CD40 plays dual roles, both activating APCs to destroy tumor stroma and driving antitumor T cell responses. To develop an optimal adaptive T cell response,

Department of Medicine, Abramson Cancer Center, University of Pennsylvania, Philadelphia, PA 19104

ORCID: 0000-0003-2702-5008 (D.L.B.).

Received for publication January 27, 2016. Accepted for publication April 28, 2016.

This work was supported by American Cancer Society Grant 125403-PF-14-135-01-LIB (to K.T.B.), National Institutes of Health Grant R01-CA-169123 (to R.H.V.), and the Pancreatic Cancer Action Network-American Association for Cancer Research (to R.H.V.).

Address correspondence and reprint requests to Dr. Robert H. Vonderheide, Abramson Cancer Center, Department of Medicine, University of Pennsylvania, 8-121 Smilow Center for Translational Research, 3400 Civic Center Boulevard, Philadelphia, PA 19104. E-mail address: rhv@exchange.upenn.edu

The online version of this article contains supplemental material.

Abbreviations used in this article: ALT, alanine aminotransferase; AST, aspartate aminotransferase; Gem, gemcitabine; HSD, honest significant difference; KPC, $Kras^{LSL-G12D/+}$, $Trp53^{LSL-R172H/+}$, $Pdx1-Cre$; MDSC, myeloid-derived suppressor cell; nP, Nab-paclitaxel; PD-1, programmed cell death-1; PDA, pancreatic ductal adenocarcinoma.

Copyright © 2016 by The American Association of Immunologists, Inc. 0022-1767/16/\$30.00

the hypothesis has been that Gem must precede anti-CD40, but given the stroma degradation observed with anti-CD40 alone, another option would be to deliver chemotherapy after anti-CD40 to potentially deliver more chemotherapy to the tumor microenvironment, which is otherwise difficult to penetrate pharmacologically (23). If this is possible, the sequence of anti-CD40 administration relative to chemotherapy may be relevant for improved treatment design.

In this study, we investigate the efficacy of anti-CD40 treatment when provided 48 h before, instead of after, standard-of-care chemotherapy for PDA. Although anti-CD40 treatment alone or after Gem therapy resulted in reduction of tumor growth as expected (16, 22), we found that pretreatment with anti-CD40 followed by Gem was lethal in half of all treated mice, regardless of whether mice were tumor bearing. Although anti-CD40 therapy recruited large numbers of myeloid cells into the liver, blockade of the inflammatory macrophage population via the administration of anti-CSF-1/IR Abs abrogated the toxicity associated with anti-CD40 pretreatment. Because anti-CD40 is being actively investigated in the clinical setting in combination with a number of treatments, including chemotherapy, these studies have implications for the design of clinical trials using anti-CD40.

Materials and Methods

Mice, tumor cell lines, and in vivo growth

The mouse pancreatic cancer cell line 4662 (CD40⁻) was generated from a C57BL/6 KPC mouse (18) as previously described (24). The genetic background of the C57BL/6 KPC mice was confirmed using the DartMouse Speed Congenic Core Facility at the Geisel School of Medicine at Dartmouth College (Hanover, NH). DartMouse uses the Illumina (San Diego, CA) GoldenGate Genotyping Assay to interrogate 1449 SNPs spread throughout the genome. The raw SNP data were analyzed using DartMouse's SNaP-Map and Map-Synth software, allowing the determination for each mouse of the genetic background at each SNP location. Wild-type C57BL/6 were purchased from Jackson Laboratory (Bar Harbor, ME). Animal protocols were reviewed and approved by the Institute of Animal Care and Use Committee at the University of Pennsylvania. PDA cells were used in experiments after three to five passages in vitro; C57BL/6 mice received 2.5×10^5 PDA cells s.c. only if viability was >94%. Cell lines were tested by using the Infectious Microbe PCR Amplification Test (IMPACT) and authenticated by the Research Animal Diagnostic Laboratory (RADL) at the University of Missouri. Tumors were measured thrice weekly by calipers, and the volume was calculated by $(L \times W^2)/2$, where L is the longest diameter and W is the perpendicular diameter. Mice were euthanized when tumor volume reached 1000 mm³.

Drug preparation

Gem (Hospira, Lake Forest, IL) pharmaceutical grade suspension at 38 mg/ml 2'-deoxy-2',2'-difluorocytidine was purchased through the Hospital of the University of Pennsylvania Pharmacy. Gem was diluted to 12 mg/ml in PBS and administered at 120 mg/kg via i.p. injection as we have previously reported (16). Nab-paclitaxel (nP; Abraxane, Celgene, Summit, NJ) pharmaceutical-grade powder was purchased through the Hospital of the University of Pennsylvania Pharmacy and resuspended at 12mg/ml in PBS. Mice received 120 mg/kg nP i.p. as previously reported (25).

mAbs

Mice received 100 or 300 µg agonist CD40 rat anti-mouse IgG2a mAb (clone FGK45), or the isotype control IgG2a mAb (clone 2A3) as previously reported (16) on day 0 (tumor-free mice), or specified day after 4662 injection. Indicated mice received 1 mg anti-CSF-1R mAb (clone AFS98) i.p. on day 6 after 4662 injection, and 0.5 mg every 3 d afterward. Some mice also received 1 mg anti-CSF-1 (clone 5A1) i.p. starting on day 6 and repeated every 3 d (26). All mAbs were purchased from BioXCell (Lebanon, NH) and were endotoxin-free.

Preparation of livers, spleen, and lungs for flow cytometry

Livers, spleen, and lungs were harvested from mice on the indicated day. Livers and lungs were minced and then incubated for 1 h in 1 mg/ml collagenase IV in DMEM at 37°C, with the addition of 50 U/ml DNase

(Roche) for lung tissues. Livers, spleen, and lungs were then mechanically dissociated and passed through a 70-µm cell strainer, incubated in ACK lysis buffer (BioWhittaker, Allendale, NJ), and used for flow cytometric analysis.

Flow cytometry

Cell surface molecules were analyzed by incubating single-cell suspensions of tissues with primary fluorochrome-labeled Abs at 4°C for 30 min in PBS with 0.5% BSA and 2 mM EDTA. Abs used in flow analysis were ordered from BD Biosciences (Sparks, MD), eBioscience (San Diego, CA) or Biolegend (San Diego, CA), and included FITC-labeled CD40 (clone HM40-3), CD45 (PE, PerCP, Alexa-Fluor 700, and QDot 605, clone 30-F11), CD115 (CSF-1R, PE, clone AFS98), CD31 (Brilliant Violet 450, clone 390), PerCP-labeled BD Viaprobe, CD11b (PerCP Cy5.5 and allophycocyanin, clone M1/70), F4/80 (PerCP, allophycocyanin Cy7, and PE Cy7, clone BM8), Gr-1 (allophycocyanin Cy7, clone RB6-8C5), CD11c (Brilliant Violet V450 or allophycocyanin, clone N418), Ly6G (allophycocyanin Cy7, clone 1A8), Ly6C (Brilliant Violet 570, clone HK1.4), and Live/Dead Aqua (Life Technologies, Carlsbad, CA). Flow cytometric analysis was performed on a FACSCanto (BD Biosciences, Sparks, MD). Collected data were analyzed using FlowJo software (Tree Star, Ashland, OR).

Immunohistochemistry

Livers, spleen, and lungs were harvested from mice 2–4 d after receiving anti-CD40 injection as indicated, and snap frozen in OCT or fixed in zinc formalin and paraffin embedded. Tissue sections were cut at 5 µm, stained with H&E, and quantified by counting all lesions visible per liver lobe at 4× magnification. Images were taken using a Nikon DS-Fi2 digital camera at 4× and 20× magnification on a Nikon Eclipse 50i and assessed at the Comparative Pathology Core at the University of Pennsylvania School of Veterinary Medicine.

Aspartate aminotransferase and alanine aminotransferase analysis

Whole blood was collected from mice sacrificed 12 h after anti-CD40 injection, and samples were tested for aspartate aminotransferase (AST) and alanine aminotransferase (ALT) by the Clinical Pathology Lab at the Ryan Veterinary Hospital at the University of Pennsylvania.

Statistical analyses

Significance of overall survival was determined using Kaplan–Meier survival curve with log-rank analysis. All other comparisons were performed using one- or two-way ANOVA with Tukey's honest significant difference (HSD) posttest or Mann–Whitney *t* test, as indicated. All statistical analyses were performed with GraphPad Prism 6 (GraphPad, La Jolla, CA). SD or SEM are as indicated by error bars. A *p* value <0.05 was considered statistically significant; **p* < 0.05, ***p* < 0.01, ****p* < 0.001, *****p* < 0.0001.

Results

CD40 agonist Ab is lethal when administered before chemotherapy

We harvested a spontaneous PDA tumor from a C57BL/6 KPC mouse and generated a cell line (4662) that upon implantation shares features with spontaneous PDA tumors, including desmoplastic stroma, extracellular matrix deposition, mutant Kras expression, and loss of p53 (24). The 4662 PDA cell line grew progressively when 2.5×10^5 cells were implanted s.c. in C57BL/6 syngeneic hosts and reached a diameter of 3–5 mm by 12 d after implantation. Treatment of mice bearing established 4662 tumors with Gem on day 12, followed by agonistic CD40 Ab on day 14 (Gem/anti-CD40), significantly reduced tumor growth rates compared with mice receiving PBS and isotype control (Fig. 1A). Tumor growth rates were also significantly reduced in mice that received the treatment regimen in reverse (anti-CD40 on day 12, followed by Gem on day 14; anti-CD40/Gem) (Fig. 1A); however, 4 of 10 mice treated with anti-CD40 followed by Gem died within 5 d of starting therapy (Fig. 1B). In comparison, 0 of 10 mice died with Gem/anti-CD40 treatment or vehicle control treatment (Fig. 1B). A similar reduction in tumor growth was observed with anti-CD40 alone (Fig. 1C), as we have previously reported (16), but there was

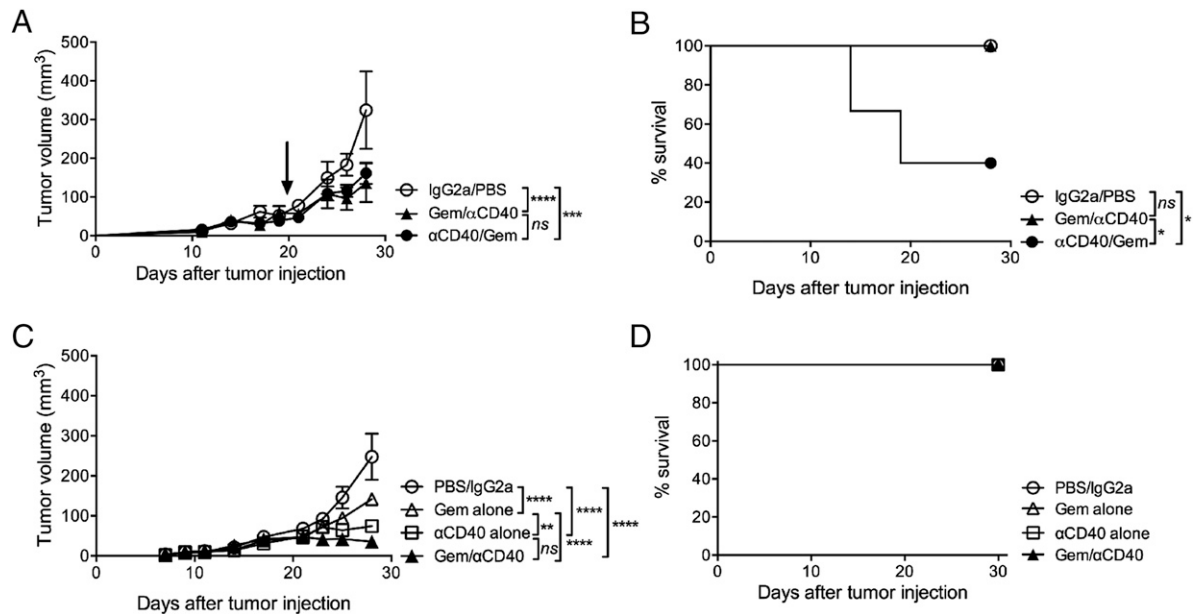


FIGURE 1. Agonistic CD40 Ab is lethal when administered before chemotherapy. Mice were injected with 4662 PDA tumor cell line and received either Gem on day 12 and anti-CD40 on day 14 (Gem/anti-CD40), or anti-CD40 on day 12 and Gem on day 14 (anti-CD40/Gem), or vehicle controls (IgG2a on day 12, PBS on day 14). **(A)** Tumor growth curves of mice treated as indicated, representative of two independent experiments, $n = 5\text{--}10$ mice/group. Arrow indicates time point at which 4/10 mice died in anti-CD40/Gem treatment group; after this time point only tumor growth on the surviving 6/10 mice is shown. **(B)** Survival curve of mice treated as indicated, from two combined experiments, $n = 5\text{--}10$ mice/group. **(C)** Tumor growth curves of mice treated as indicated including Gem alone or anti-CD40 alone on day 12, representative of two independent experiments, $n = 6$ mice/group. **(D)** Survival curve of mice from (C). Statistical analysis by two-way ANOVA with Tukey's HSD posttest (A and C) or by Kaplan-Meier (B and D). Each symbol represents a group of mice; error bars indicate SEM. * $p < 0.05$, *** $p < 0.001$, **** $p < 0.0001$. ns, not significant.

no lethal toxicity with anti-CD40 alone, Gem alone, or Gem followed by CD40 (Fig. 1D). After treatment with either anti-CD40 or Gem alone, 0 of 12 mice died across two independent experiments, and we have previously reported the safety of these drugs as monotherapies (16). But across 10 independent experiments, 46 of 82 (56%) mice treated with anti-CD40 followed by Gem died, compared with 0 of 22 mice after Gem/anti-CD40 in 4 experiments and 0 of 14 mice after IgG2a/PBS in 3 experiments.

To determine whether the presence of a growing tumor was required for lethal sensitivity to anti-CD40/Gem therapy, we treated tumor-free C57BL/6 mice with anti-CD40/Gem; survival rates were similar to those observed in anti-CD40/Gem mice bearing established tumors (Fig. 2A), and across 6 experiments, 11 of 34 (32.2%) tumor-free mice died after anti-CD40/Gem treatment. To investigate the potential for dose-mediated lethality after anti-CD40/Gem treatment, we increased the amount of anti-CD40 administered to mice from 100 to 300 μg but found that survival rates were similar in mice regardless of the amount of anti-CD40 received before Gem administration (Fig. 2B). Across 15 experiments, with both tumor-bearing and tumor-free mice, 56 of 124 (45.2%) mice treated with 300 μg anti-CD40 followed by Gem died, compared with 57 of 98 (58.1%) mice treated with 100 μg anti-CD40 followed by Gem (data not shown). We did not test lower doses of anti-CD40 in these experiments because we have previously observed that lower doses fail to demonstrate a pharmacodynamic effect.

Given that both mice and patients can be successfully treated with Gem 5 d after anti-CD40 as part of a combination therapeutic schema (16), we next investigated the time frame in which Gem administration after anti-CD40 treatment is lethal. Although the administration of Gem 2 d after anti-CD40 is toxic in 56% of treated mice (Fig. 1), Gem administration 3 or 4 d after anti-CD40 was not lethal to mice (Fig. 2C). Furthermore, when substituting nP (Abraxane), a different chemotherapy but also Food and Drug

Administration approved for PDA, the combination was also toxic when nP was administered within 2 d after anti-CD40 and remained lethal even on day 3 (Fig. 2D). Hence there is a temporal window after anti-CD40 administration when treatment with chemotherapy significantly reduces the survival of treated mice.

Agonistic CD40 stimulation combined with chemotherapy drives hepatotoxicity

Given that a subset of mice were dying 2 d after completing anti-CD40/Gem therapy, cohorts of mice were sacrificed 48 h after the completion of treatment to investigate causality. Pathologic lesions were grossly observed in liver parenchyma and on the capsule of anti-CD40/Gem-treated mice that were not present in the livers of Gem/anti-CD40-treated mice (Fig. 3A, lesions indicated by arrow). No other pathological findings were noted on gross inspection. The number of lesions observed per lobe of liver using H&E staining was significantly higher in mice treated with anti-CD40/Gem (mean 2.9 ± 0.6) as compared with mice with Gem/anti-CD40 (mean 0.2 ± 0.2 , $p < 0.01$) (Fig. 3B). Microscopically, livers from both anti-CD40/Gem- and Gem/anti-CD40-treated mice exhibited coagulative hepatocellular necrosis compared with IgG2a/PBS control-treated mice, primarily surrounding veins (both central and portal) and frequently associated with occlusive to partially occlusive fibrin thrombi (Fig. 3C). These findings are consistent with infarcts, with the likely cause of death in anti-CD40/Gem-treated mice being multiple hepatic infarcts. However, moderate-to-severe multifocal granulomatous and neutrophilic infiltrates were observed in all mice treated with anti-CD40/Gem (14/14), whereas only 2 of 5 mice treated with Gem/anti-CD40 were found to have minimal to mild granulomatous and neutrophilic infiltrates. Assessment of both the spleen and the lung at the same time point revealed no macroscopic lesions at the time of sacrifice, and upon histopathological examination, no evidence of necrosis within the tissues, although three of five mice treated with

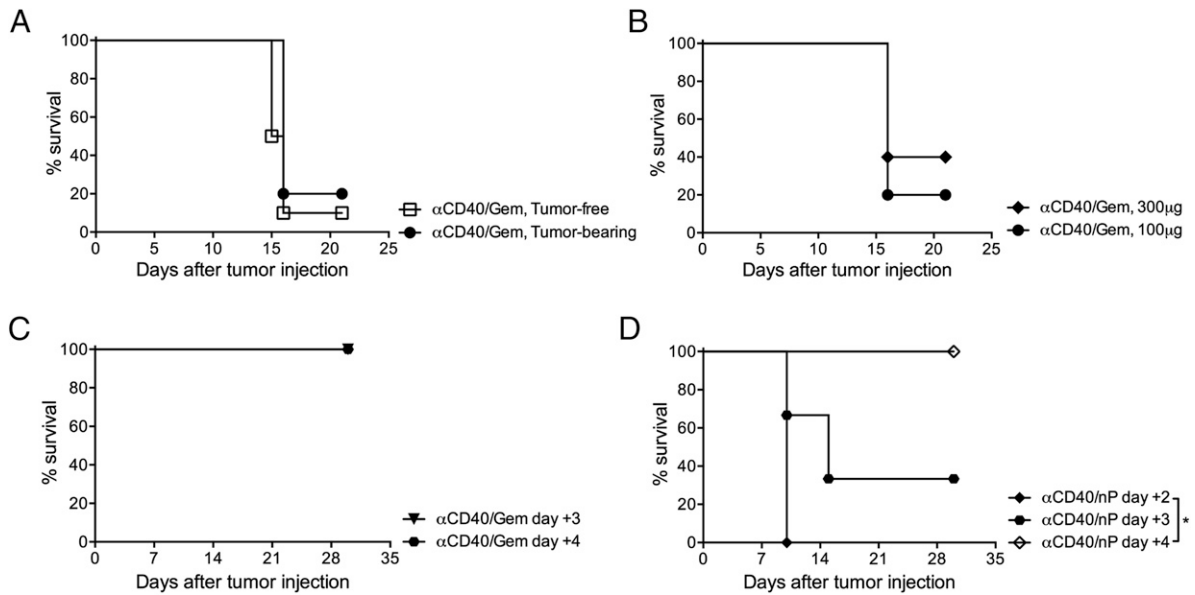


FIGURE 2. Chemotherapy is toxic when administered 2 d after anti-CD40 therapy, regardless of tumor-bearing status of the host. **(A)** Mice were injected with 4662 PDA tumor cells (tumor-bearing) or left uninjected (tumor-free) on day 0, and received anti-CD40 on day 11 and Gem on day 13. Survival curve is representative of 4 experiments, 5–10 mice/group. **(B)** Mice were treated as described in Fig. 1, except that tumor-bearing mice received either 100 or 300 μg anti-CD40 on day 11 as indicated, followed by Gem on day 13. Survival representative of two experiments, $n = 5$ mice/group. **(C)** Mice were treated as described in Fig. 1, except that Gem was administered 3 or 4 d after anti-CD40, as indicated. Survival curve representative of two experiments, $n = 3$ –5 mice/group. **(D)** Mice were treated as described in Fig. 1, except that mice received nP instead of Gem on 2, 3, or 4 d, as indicated, after anti-CD40 treatment, $n = 3$ mice/group. Each symbol represents a group of mice. Statistical analyses by Kaplan–Meier ($*p < 0.05$).

anti-CD40/Gem were observed to have minimal multifocal lymphohistiocytic perivascular infiltrates in the lung. In addition, 3 of 20 mice treated with anti-CD40 \pm Gem presented with capillary fibrin thrombi in the lung, associated with the systemic hypercoagulable state observed in the liver tissue.

To quantify further the magnitude of hepatotoxicity after anti-CD40/Gem therapy, we determined serum levels of ALT and AST 12 h after the completion of treatment in all cohorts of mice. Both ALT and AST levels were significantly increased (628.7 ± 267.4 and 918.7 ± 391 U/l, respectively) in mice receiving anti-CD40/Gem compared with Gem/anti-CD40 (140 ± 4.4 and 133.7 ± 10.2 U/l) or vehicle controls (136 ± 11.9 and 102.3 ± 19.9 U/l) (Fig. 3D), revealing that the administration of anti-CD40 followed by Gem results in rapid and significant liver damage in mice.

CD40 stimulation increases activated myeloid populations in the liver

Given the hepatotoxicity caused by anti-CD40/Gem and that anti-CD40 stimulates APCs, including dendritic cells and macrophages (16), we hypothesized that anti-CD40 was activating APCs within the liver compartment. Indeed, 24 h after anti-CD40, the overall proportion of total CD11b⁺ myeloid cells in the liver was significantly increased to 36.4%, as was the frequency of CD11b⁺ Gr1⁺ neutrophils/myeloid-derived suppressor cells (MDSCs) (21.6%), compared with IgG2a/PBS vehicle control treatment (from 6.2% myeloid cells and 1.4% MDSCs, respectively) (Fig. 4A, top and middle panels). Conversely, the total frequency of F4/80⁺ macrophages was significantly decreased in the livers of mice treated with anti-CD40: 9.8 versus 17.5% in control-treated mice (Fig. 4A, bottom panel).

The proportion of activated CD86⁺ MHCII⁺ CD11b⁺ cells was significantly increased in the livers of anti-CD40–treated mice (mean 18.9 versus 8.9% in control-treated mice), as were the frequencies of activated MDSCs, although to a lesser extent (mean 13.8 versus 9.3% in control-treated mice) (Fig. 4B, top and middle

panels). Although the frequency of the total macrophage population was reduced, the frequency of activated macrophages, as measured by the proportion of CD86⁺ MHCII⁺ F4/80⁺ cells, was significantly increased after anti-CD40 (mean 65.9 versus 1.4% in control-treated mice) (Fig. 4B, bottom panel). In addition, even though nearly 70% of F4/80⁺ macrophages were CD40⁺, stimulation with anti-CD40 further increased CD40⁺ expression (mean 85.5 versus 65.9% in control-treated mice, mean fluorescence intensity 2795 ± 321 in anti-CD40–treated mice versus 1345 ± 258 in control-treated mice). In comparison, activated myeloid cells and MDSCs exhibited no significant alterations in the proportion of CD40⁺ cells after anti-CD40 treatment (Fig. 4C). Furthermore, the expression of CD40 on CD45[−] cells, including hepatocytes and vascular endothelial cells known to express CD40 (27–29), was not increased after anti-CD40 therapy (Fig. 4D). The changes in the hepatic myeloid subsets were observed only within the relative frequencies of cells, because the absolute cell numbers per gram of liver were not significantly different across groups (Supplemental Fig. 1), potentially because of alterations in the frequencies of other (nonmyeloid) leukocyte subsets. Furthermore, treatment with anti-CD40 resulted in splenomegaly regardless of the timing of Gem administration (Supplemental Fig. 2A, 2B), associated with moderate-to-severe white pulp hyperplasia as a result of systemic immune activation (Supplemental Fig. 2C). The total splenic myeloid cell population per gram of tissue was significantly reduced after anti-CD40 therapy, as well as both monocytic (Mo-) and granulocytic (G-) MDSCs in mice treated with anti-CD40/Gem (Supplemental Fig. 2D, 2E). A slight increase in the proportion of CD40⁺ Mo-MDSCs was observed in the lungs of anti-CD40/Gem–treated mice compared with vehicle control-treated mice, but no other obvious alterations in myeloid cell subsets were observed (Supplemental Fig. 3). Thus, anti-CD40 therapy primarily alters the hepatic myeloid cell compartment and significantly increases the frequency of activated, mature macrophages within the liver after treatment.

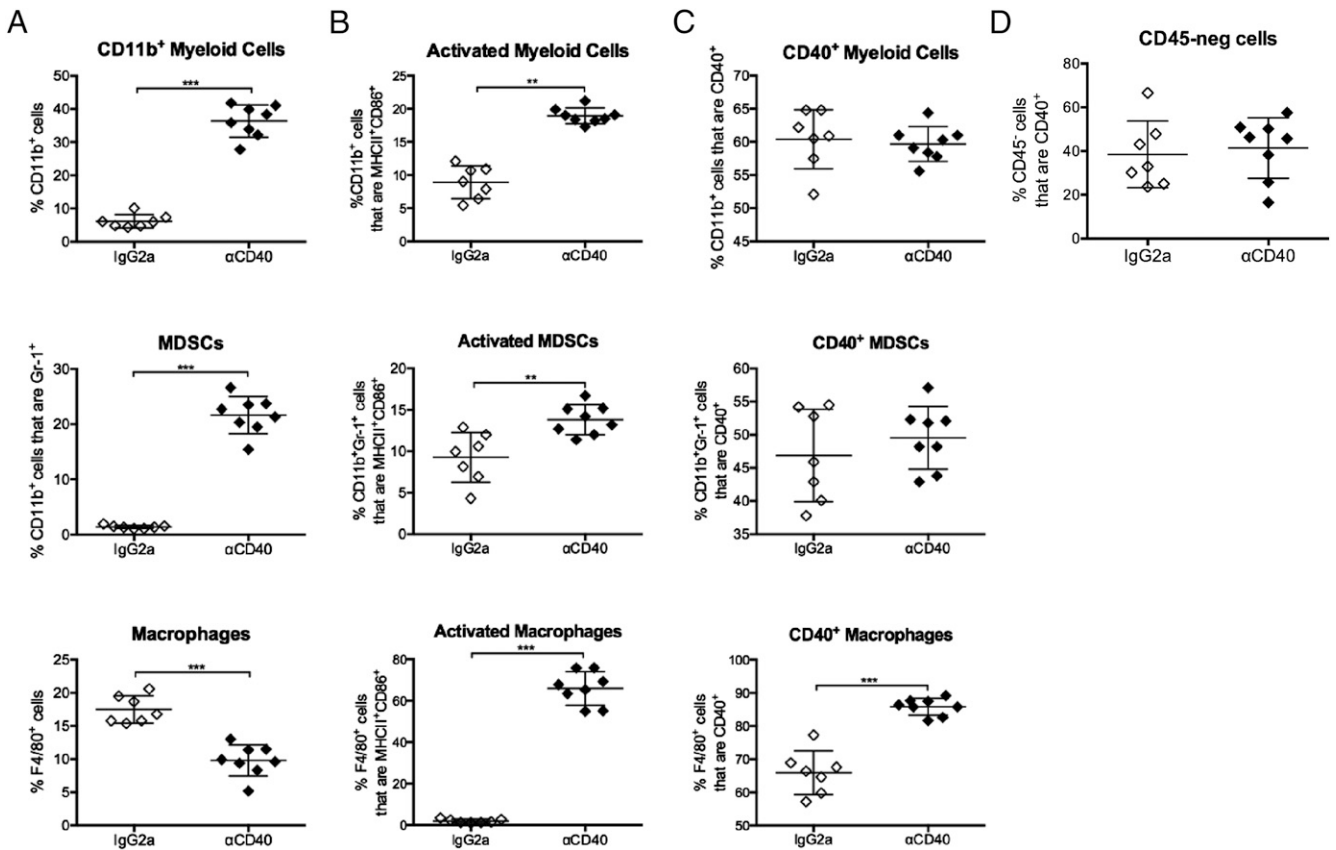


FIGURE 4. Anti-CD40 therapy increases the frequency of activated macrophages in the livers of treated mice. Mice were treated with anti-CD40 and sacrificed 1 d after treatment. Livers were harvested and analyzed by flow cytometry with regard to the indicated cell populations among live CD45⁺ cells (**A–C**) or live CD45[−] cells (**D**). Each symbol represents an individual mouse, horizontal bars indicate mean, and error bars indicate SD; data are representative of two independent experiments with $n = 5–8$ mice/group. Statistical analysis by Mann–Whitney unpaired t test, * $p < 0.05$, ** $p < 0.01$, *** $p < 0.001$.

CD40/Gem and anti-CSF-1R exhibited moderate multifocal acute coagulative hepatocellular necrosis (with two of four mild and one of four minimal). Furthermore, the livers from anti-CD40/Gem-treated mice had widely dispersed hepatocyte necrosis, which was individualized and had indistinct margins, compared with livers from anti-CD40/Gem + anti-CSF-1R-treated mice, for which the coagulative necrosis was observed in confluent areas with clear distinction between normal and necrotic hepatocytes. No necrotic foci were noted in the spleen of mice treated with anti-CD40/Gem ± anti-CSF-1R, despite an increase in spleen weight with anti-CSF-1R alone (Supplemental Fig. 4A). Thus, blocking CSF-1R abrogates many of the hepatotoxic histopathological effects observed with anti-CD40/Gem treatment.

To determine the cell populations targeted by anti-CSF-1R mAbs, and mediating the hepatotoxicity of anti-CD40/Gem, we performed flow cytometry on livers 24 h after anti-CD40 treatment. A significant reduction in the frequencies of activated macrophages was observed in the livers of mice treated with CD40 and CSF-1/1R mAb (Fig. 5D, 5E). The proportions of both CD40⁺ F4/80⁺ macrophages and CD86⁺ MHCII⁺ F4/80⁺ macrophages were increased with anti-CD40 and reduced to frequencies similar to IgG2a-treated mice with the addition of anti-CSF-1/1R mAbs (Fig. 5D, 5E, respectively). Despite previous studies reporting a major role of MDSCs in mediating CD40 hepatotoxicity in the absence of chemotherapy (30), the proportion of MDSCs in the livers of anti-CD40-treated mice receiving anti-CSF-1/1R were not altered (Fig. 5F), in agreement with increased CSF-1R expression on macrophages, but not MDSC subsets, in the livers of anti-CD40/Gem-treated mice (Supplemental Fig.

4B). Nevertheless, the frequency of F4/80⁺ CD11b⁺ Gr1⁺ cells was significantly reduced after treatment with anti-CD40/Gem ± anti-CSF-1R (Supplemental Fig. 4C). The frequency and total number of both Mo- and G-MDSC subsets per gram of liver in mice treated with anti-CD40/Gem were not significantly altered with the addition of anti-CSF-1R (Supplemental Fig. 4D, 4E). Furthermore, the proportion of CD40⁺ CD45[−] cells, including hepatocytes, was also not significantly altered after anti-CD40/Gem and anti-CSF-1R treatment (Fig. 5G). Instead, these data reveal that activated macrophages mediate liver damage after anti-CD40/Gem administration, and inhibiting macrophage activation via CSF-1R blockade abrogated liver toxicity and significantly inhibited tumor growth and enhanced overall survival.

Discussion

The success of immunotherapies in tumors replete with T cell infiltration is in stark contrast with the failure of the same treatments in T cell-poor tumors such as PDA. Anti-CD40 is capable of converting immunotherapy-resistant tumors susceptible to T cell infiltration and destruction, but the requirement of concomitant therapies, such as chemotherapy, is poorly understood. In this study, in a mouse model of PDA, we show that anti-CD40 therapy can inhibit tumor growth but causes significant and lethal hepatotoxicity when administered 48 h in advance of (instead of after) Gem, regardless of the tumor-bearing status of the mouse. Anti-CD40 treatment significantly increased the proportion of activated macrophages within the liver, and blockade of macrophage activation using anti-CSF-1/1R mAbs abrogated the lethality of anti-CD40/Gem treatment without reducing the antitumor efficacy

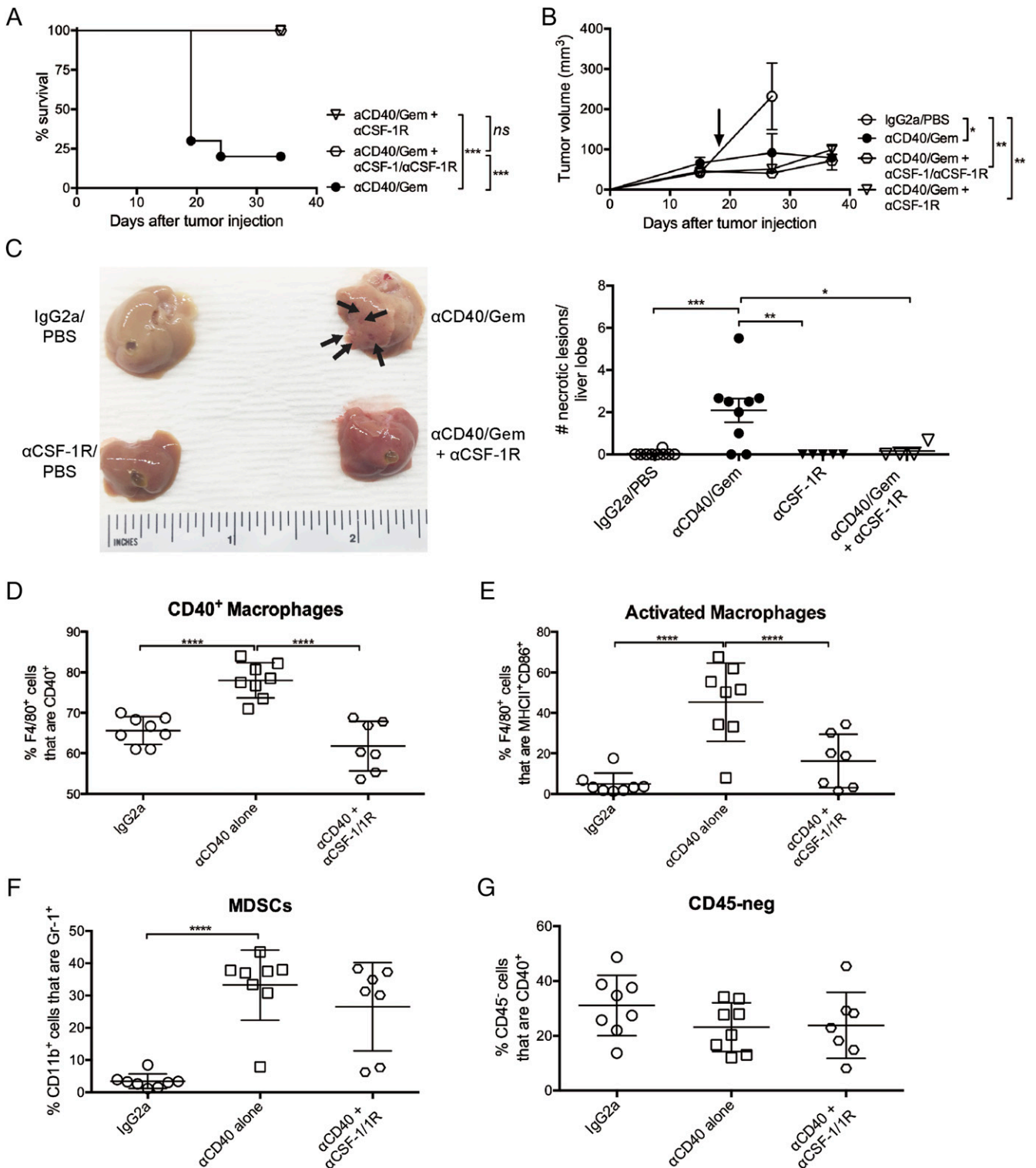


FIGURE 5. Blockade of macrophage activation abrogates hepatotoxicity of anti-CD40/Gem treatment. Mice were treated as described in Fig. 1, except some mice also received anti-CSF-1 and/or anti-CSF-1R starting on day 6 and repeated every 3 d for the duration of the experiment. **(A and B)** Survival curve (A) or tumor growth kinetics (B) of mice treated with anti-CD40/Gem or anti-CD40/Gem with anti-CSF-1 and/or anti-CSF-1R. Data are representative of three independent experiments with $n = 4-10$ mice/group, and from two combined experiments (*right panel*). Each symbol represents a group of mice, error bars indicate mean \pm SEM, and arrow indicates time point when 7/19 mice died in anti-CD40/Gem-treated group. **(C)** Mice were treated as in (A), except that mice were sacrificed on day 16. *Left panel*, Representative livers from indicated treatment groups with macroscopic lesions indicated by arrows. *Right panel*, Quantification of lesions observed at 4 \times original magnification per lobe of liver for indicated groups, from two combined experiments with $n = 4-5$ mice/group. **(D-G)** Mice were euthanized on day 12, and livers were analyzed by flow cytometry with regard to the indicated cell populations among live CD45⁺ cells (D-F) or live CD45⁻ cells (G). Each symbol represents a single mouse, $n = 7-8$ mice/group; data are representative of two independent experiments. Horizontal line indicates mean \pm SD. Statistical analyses by Kaplan-Meier (A), two-way ANOVA (B), or one-way ANOVA with Tukey's HSD posttest (C-G). * $p < 0.05$, ** $p < 0.01$, *** $p < 0.001$, **** $p < 0.0001$.

of the combination treatment. The data presented in this article highlight at once the potency of anti-CD40 therapy to activate both innate and adaptive immunity and also important pharmacological limitations with regard to sequencing with chemotherapy. These studies have implications for the design of upcoming clinical trials investigating anti-CD40–chemotherapy combinations in cancer.

CD40 Ab has been administered to patients in a number of clinical trials with minimal adverse events (31–34), but the murine studies herein reveal a previously unrecognized temporal window after anti-CD40 administration during which chemotherapy should not be administered. We have found that separating anti-CD40 and subsequent Gem administration by 5 d is safe in both mouse models and patients with PDA (16). However, administration of Gem or nP only 2 or 3 d after anti-CD40 resulted in significant and lethal hepatotoxicity, and was likely the cause of treatment-related deaths in mice after repeated doses of Gem and anti-CD40 in overlapping treatment schedules (17). This finding is despite the fact that Gem therapy rarely results in liver damage in patients with PDA (35), non–small cell lung cancer (36), or other tumor types (37), and that anti-CD40 therapy as a single agent has been reported to drive only mild, transient, and nonlethal hepatotoxicity in mice (30, 38) and humans (34). However, anti-CD40 combined with IL-2 has also been reported to result in lethal hepatotoxicity in tumor-bearing mice (39, 40), indicating that the potency of anti-CD40 needs to be considered in all combinatorial treatments, not only those with chemotherapy. These studies highlight the need for understanding the context and timing of combination therapies for the safe use of anti-CD40. Our data support the need for careful sequential administration of anti-CD40 *after*, not before, chemotherapy, in the absence of macrophage modulation. This finding is important because the stroma depletion caused by anti-CD40 alone (16) might have otherwise been considered a useful first maneuver to improve the delivery of increased concentrations of chemotherapy to highly desmoplastic tumors, thereby overcoming chemotherapy resistance in PDA.

Mechanistic studies to determine the cells mediating hepatotoxicity after anti-CD40/Gem revealed a role for activated macrophages, similar to what has been shown in hepatotoxicity observed after anti-CD40/IL-2 in aged or obese mice (39, 40). Although MDSCs were increased in the liver after anti-CD40, the frequency of MDSCs was unaltered after anti-CSF-1/1R therapy, even though hepatotoxicity was resolved. We also found no significant alterations after anti-CSF-1/1R therapy within the CD45⁺ cellular compartment, which includes hepatocytes and vascular endothelial cells, despite previous reports that CD40–ligand stimulation of hepatocytes promotes the upregulation of CD40 by the hepatocytes and exacerbation of fulminant hepatitis in a FasL-dependent manner (28, 29). The high frequency of occlusive hepatic infarcts in anti-CD40/Gem-treated mice is consistent with the significant role for CD40 in two mouse models of thrombosis (41) in which macrophages are strongly activated, similar to anti-CD40 treatment. In anti-CD40/Gem-treated mice, liver damage is CSF-1R dependent and can be alleviated via blockade of macrophage activation using anti-CSF-1/1R mAbs.

The fact that blunted macrophage activation did not alter the antitumor efficacy in anti-CD40/Gem-treated mice is in contrast with our previous work identifying a major role for anti-CD40–induced tumoricidal macrophages in mediating tumor regressions of spontaneous PDA tumors in KPC mice (16). Although macrophages mediated anti-CD40–induced antitumor immunity as a single agent, in the absence of Gem, T cell immunity did not develop with this treatment (16). However, T cell immunity against PDA is generated when anti-CD40 is administered subsequent to Gem (22), and

is further potentiated by the addition of nP, as well as anti-PD-1/anti-CTLA-4 (21). Thus, the approach in which anti-CD40 therapy is used can significantly alter the dominant mechanism of antitumor immune activation, switching between innate and adaptive immune-mediated tumor regressions depending on the presence or absence of chemotherapy. Although reversing the treatment schedule by providing anti-CD40 before Gem successfully increased the activity of innate immune cells during treatment, the activated macrophages mediated liver damage. Blocking macrophage activation via anti-CSF-1/1R mAbs prevented lethal hepatotoxicity without further enhancement (or reduction) of antitumor immunity. Indeed, in the absence of anti-CD40 treatment, anti-CSF-1/1R mAbs have been shown to contribute to the reprogramming of macrophages in the PDA tumor microenvironment rendering the tumor sensitive to immune checkpoint blockade therapies (26). Thus, anti-CD40/Gem with anti-CSF-1/1R and anti-PD-1/anti-CTLA-4 may be a highly effective therapy that can be investigated in future studies.

The important opportunity for using immunotherapies for patients with cancer is clear, and identifying treatments that can generate effective T cell responses in cancers currently resistant to newly approved immune interventions is of high priority. Our studies in this article build upon the identification of anti-CD40 as a potent activator of antitumor immunity in both preclinical and clinical studies. However, our finding that anti-CD40 can be hepatotoxic and lethal when administered in advance of chemotherapy reveals the need to continue investigating anti-CD40 combinations in preclinical studies. These data provide key information to design safe anti-CD40 clinical trials, maintaining the ability to harness the potential of anti-CD40 in cancer therapies whereas minimizing potential toxicity.

Acknowledgments

We thank Drs. Elizabeth Buza and Amy Durham from the Abramson Cancer Center Comparative Pathology Core at the University of Pennsylvania School of Veterinary Medicine for assistance with samples.

Disclosures

The authors have no financial conflicts of interest.

References

1. Brahmer, J. R., S. S. Tykodi, L. Q. Chow, W. J. Hwu, S. L. Topalian, P. Hwu, C. G. Drake, L. H. Camacho, J. Kauh, K. Odunsi, et al. 2012. Safety and activity of anti-PD-L1 antibody in patients with advanced cancer. *N. Engl. J. Med.* 366: 2455–2465.
2. Hodi, F. S., S. J. O'Day, D. F. McDermott, R. W. Weber, J. A. Sosman, J. B. Haanen, R. Gonzalez, C. Robert, D. Schadendorf, J. C. Hassel, et al. 2010. Improved survival with ipilimumab in patients with metastatic melanoma. *N. Engl. J. Med.* 363: 711–723.
3. Robert, C., J. Schachter, G. V. Long, A. Arance, J. J. Grob, L. Mortier, A. Daud, M. S. Carlino, C. McNeil, M. Lotem, et al; KEYNOTE-006 Investigators. 2015. Pembrolizumab versus ipilimumab in advanced melanoma. *N. Engl. J. Med.* 372: 2521–2532.
4. Sharma, P., and J. P. Allison. 2015. Immune checkpoint targeting in cancer therapy: toward combination strategies with curative potential. *Cell* 161: 205–214.
5. Tumeh, P. C., C. L. Harview, J. H. Yearley, I. P. Shintaku, E. J. Taylor, L. Robert, B. Chmielowski, M. Spasic, G. Henry, V. Ciobanu, et al. 2014. PD-1 blockade induces responses by inhibiting adaptive immune resistance. *Nature* 515: 568–571.
6. Sausen, M., J. Phallen, V. Adleff, S. Jones, R. J. Leary, M. T. Barrett, V. Anagnostou, S. Parpart-Li, D. Murphy, Q. Kay Li, et al. 2015. Clinical implications of genomic alterations in the tumour and circulation of pancreatic cancer patients. *Nat. Commun.* 6: 7686.
7. Jones, S., X. Zhang, D. W. Parsons, J. C. Lin, R. J. Leary, P. Angenendt, P. Mankoo, H. Carter, H. Kamiyama, A. Jimeno, et al. 2008. Core signaling pathways in human pancreatic cancers revealed by global genomic analyses. *Science* 321: 1801–1806.
8. Alexandrov, L. B., S. Nik-Zainal, D. C. Wedge, S. A. J. R. Aparicio, S. Behjati, A. V. Biankin, G. R. Bignell, N. Bolli, A. Borg, A.-L. Børresen-Dale, et al. 2013. Signatures of mutational processes in human cancer. *Nature* 500: 415–421.
9. Burris, H. A., III, M. J. Moore, J. Andersen, M. R. Green, M. L. Rothenberg, M. R. Modiano, M. C. Cripps, R. K. Portenoy, A. M. Storniolo, P. Tarassoff, et al. 1997. Improvements in survival and clinical benefit with gemcitabine as first-line therapy for patients with advanced pancreas cancer: a randomized trial. *J. Clin. Oncol.* 15: 2403–2413.

10. Le, D. T., E. Lutz, J. N. Uram, E. A. Sugar, B. Onners, S. Solt, L. Zheng, L. A. Diaz, Jr., R. C. Donehower, E. M. Jaffee, and D. A. Laheru. 2013. Evaluation of ipilimumab in combination with allogeneic pancreatic tumor cells transfected with a GM-CSF gene in previously treated pancreatic cancer. *J. Immunother.* 36: 382–389.
11. Royal, R. E., C. Levy, K. Turner, A. Mathur, M. Hughes, U. S. Kammula, R. M. Sherry, S. L. Topalian, J. C. Yang, I. Lowy, and S. A. Rosenberg. 2010. Phase 2 trial of single agent Ipilimumab (anti-CTLA-4) for locally advanced or metastatic pancreatic adenocarcinoma. *J. Immunother.* 33: 828–833.
12. Bennett, S. R., F. R. Carbone, F. Karamalis, R. A. Flavell, J. F. Miller, and W. R. Heath. 1998. Help for cytotoxic-T-cell responses is mediated by CD40 signalling. *Nature* 393: 478–480.
13. Schoenberger, S. P., R. E. Toes, E. I. van der Voort, R. Offringa, and C. J. Melief. 1998. T-cell help for cytotoxic T lymphocytes is mediated by CD40-CD40L interactions. *Nature* 393: 480–483.
14. Ridge, J. P., F. Di Rosa, and P. Matzinger. 1998. A conditioned dendritic cell can be a temporal bridge between a CD4+ T-helper and a T-killer cell. *Nature* 393: 474–478.
15. Sotomayor, E. M., I. Borrello, E. Tubb, F. M. Rattis, H. Bien, Z. Lu, S. Fein, S. Schoenberger, and H. I. Levitsky. 1999. Conversion of tumor-specific CD4+ T-cell tolerance to T-cell priming through in vivo ligation of CD40. *Nat. Med.* 5: 780–787.
16. Beatty, G. L., E. G. Chiorean, M. P. Fishman, B. Saboury, U. R. Teitelbaum, W. Sun, R. D. Huhn, W. Song, D. Li, L. L. Sharp, et al. 2011. CD40 agonists alter tumor stroma and show efficacy against pancreatic carcinoma in mice and humans. *Science* 331: 1612–1616.
17. Nowak, A. K., B. W. Robinson, and R. A. Lake. 2003. Synergy between chemotherapy and immunotherapy in the treatment of established murine solid tumors. *Cancer Res.* 63: 4490–4496.
18. Hingorani, S. R., L. Wang, A. S. Multani, C. Combs, T. B. Deramaudt, R. H. Hruban, A. K. Rustgi, S. Chang, and D. A. Tuveson. 2005. Trp53R172H and KrasG12D cooperate to promote chromosomal instability and widely metastatic pancreatic ductal adenocarcinoma in mice. *Cancer Cell* 7: 469–483.
19. Westcott, P. M., K. D. Halliwill, M. D. To, M. Rashid, A. G. Rust, T. M. Keane, R. Delrosario, K. Y. Jen, K. E. Gurley, C. J. Kemp, et al. 2015. The mutational landscapes of genetic and chemical models of Kras-driven lung cancer. *Nature* 517: 489–492.
20. Clark, C. E., S. R. Hingorani, R. Mick, C. Combs, D. A. Tuveson, and R. H. Vonderheide. 2007. Dynamics of the immune reaction to pancreatic cancer from inception to invasion. *Cancer Res.* 67: 9518–9527.
21. Winograd, R., K. T. Byrne, R. A. Evans, P. M. Odorizzi, A. R. Meyer, D. L. Bajor, C. Clendenin, B. Z. Stanger, E. E. Furth, E. J. Wherry, and R. H. Vonderheide. 2015. Induction of T-cell immunity overcomes complete resistance to PD-1 and CTLA-4 blockade and improves survival in pancreatic carcinoma. *Cancer Immunol. Res.* 3: 399–411.
22. Beatty, G. L., R. Winograd, R. A. Evans, K. B. Long, S. L. Luque, J. W. Lee, C. Clendenin, W. L. Gladney, D. M. Knoblock, P. D. Guirnalda, and R. H. Vonderheide. 2015. Exclusion of T cells from pancreatic carcinomas in mice is regulated by Ly6C(low) F4/80(+) extratumoral macrophages. *Gastroenterology* 149: 201–210.
23. Olive, K. P., M. A. Jacobetz, C. J. Davidson, A. Gopinathan, D. McIntyre, D. Honess, B. Madhu, M. A. Goldgraben, M. E. Caldwell, D. Allard, et al. 2009. Inhibition of Hedgehog signaling enhances delivery of chemotherapy in a mouse model of pancreatic cancer. *Science* 324: 1457–1461.
24. Lo, A., L. C. Wang, J. Scholler, J. Monslow, D. Avery, K. Newick, S. O'Brien, R. A. Evans, D. J. Bajor, C. Clendenin, et al. 2015. Tumor-promoting desmoplasia is disrupted by depleting FAP-expressing stromal cells. *Cancer Res.* 75: 2800–2810.
25. Frese, K. K., A. Neesse, N. Cook, T. E. Bapiro, M. P. Lolkema, D. I. Jodrell, and D. A. Tuveson. 2012. nab-Paclitaxel potentiates gemcitabine activity by reducing cytidine deaminase levels in a mouse model of pancreatic cancer. *Cancer Discov.* 2: 260–269.
26. Zhu, Y., B. L. Knolhoff, M. A. Meyer, T. M. Nywening, B. L. West, J. Luo, A. Wang-Gillam, S. P. Goedegebuure, D. C. Linehan, and D. G. DeNardo. 2014. CSF1/CSF1R blockade reprograms tumor-infiltrating macrophages and improves response to T-cell checkpoint immunotherapy in pancreatic cancer models. *Cancer Res.* 74: 5057–5069.
27. Hollenbaugh, D., N. Mischel-Petty, C. P. Edwards, J. C. Simon, R. W. Denfeld, P. A. Kiener, and A. Aruffo. 1995. Expression of functional CD40 by vascular endothelial cells. *J. Exp. Med.* 182: 33–40.
28. Afford, S. C., S. Randhawa, A. G. Eliopoulos, S. G. Hubscher, L. S. Young, and D. H. Adams. 1999. CD40 activation induces apoptosis in cultured human hepatocytes via induction of cell surface fas ligand expression and amplifies fas-mediated hepatocyte death during allograft rejection. *J. Exp. Med.* 189: 441–446.
29. Zhou, F., M. N. Ajuebor, P. L. Beck, T. Le, C. M. Hogaboam, and M. G. Swain. 2005. CD154-CD40 interactions drive hepatocyte apoptosis in murine fulminant hepatitis. *Hepatology* 42: 372–380.
30. Medina-Echeverez, J., C. Ma, A. G. Duffy, T. Eggert, N. Hawk, D. E. Kleiner, F. Korangy, and T. F. Greten. 2015. Systemic agonistic anti-CD40 treatment of tumor-bearing mice modulates hepatic myeloid-suppressive cells and causes immune-mediated liver damage. *Cancer Immunol. Res.* 3: 557–566.
31. Vonderheide, R. H., and M. J. Glennie. 2013. Agonistic CD40 antibodies and cancer therapy. *Clin. Cancer Res.* 19: 1035–1043.
32. Melero, I., S. Hervas-Stubb, M. Glennie, D. M. Pardoll, and L. Chen. 2007. Immunostimulatory monoclonal antibodies for cancer therapy. *Nat. Rev. Cancer* 7: 95–106.
33. Bajor, D. L., X. Xu, D. A. Torigian, R. Mick, L. R. Garcia, L. P. Richman, C. Desmarais, K. L. Nathanson, L. M. Schuchter, M. Kalos, and R. H. Vonderheide. 2014. Immune activation and a 9-year ongoing complete remission following CD40 antibody therapy and metastasectomy in a patient with metastatic melanoma. *Cancer Immunol. Res.* 2: 1051–1058.
34. Vonderheide, R. H., K. T. Flaherty, M. Khalil, M. S. Stumacher, D. L. Bajor, N. A. Hutnick, P. Sullivan, J. J. Mahany, M. Gallagher, A. Kramer, et al. 2007. Clinical activity and immune modulation in cancer patients treated with CP-870,893, a novel CD40 agonist monoclonal antibody. *J. Clin. Oncol.* 25: 876–883.
35. Carmichael, J., U. Fink, R. C. Russell, M. F. Spittle, A. L. Harris, G. Spiessi, and J. Blatter. 1996. Phase II study of gemcitabine in patients with advanced pancreatic cancer. *Br. J. Cancer* 73: 101–105.
36. Anderson, H., B. Lund, F. Bach, N. Thatcher, J. Walling, and H. H. Hansen. 1994. Single-agent activity of weekly gemcitabine in advanced non-small-cell lung cancer: a phase II study. *J. Clin. Oncol.* 12: 1821–1826.
37. Green, M. R. 1996. Gemcitabine safety overview. *Semin. Oncol.* 23(5Suppl. 10): 32–35.
38. Fransen, M. F., M. Sluiter, H. Morreau, R. Arens, and C. J. Melief. 2011. Local activation of CD8 T cells and systemic tumor eradication without toxicity via slow release and local delivery of agonistic CD40 antibody. *Clin. Cancer Res.* 17: 2270–2280.
39. Bouchlaka, M. N., G. D. Sckisel, M. Chen, A. Mirsoian, A. E. Zamora, E. Maverakis, D. E. Wilkins, K. L. Alderson, H. H. Hsiao, J. M. Weiss, et al. 2013. Aging predisposes to acute inflammatory induced pathology after tumor immunotherapy. *J. Exp. Med.* 210: 2223–2237.
40. Mirsoian, A., M. N. Bouchlaka, G. D. Sckisel, M. Chen, C. C. Pai, E. Maverakis, R. G. Spencer, K. W. Fishbein, S. Siddiqui, A. M. Monjazeb, et al. 2014. Adiposity induces lethal cytokine storm after systemic administration of stimulatory immunotherapy regimens in aged mice. *J. Exp. Med.* 211: 2373–2383.
41. Gavins, F. N., G. Li, J. Russell, M. Perretti, and D. N. Granger. 2011. Microvascular thrombosis and CD40/CD40L signaling. *J. Thromb. Haemost.* 9: 574–581.